

Estimation of Multidimensional Precipitation Parameters by Areal Estimates of Oceanic Rainfall

J. B. VALDÉS,¹ S. NAKAMOTO,² S. S. P. SHEN,³ AND G. R. NORTH²

The parameters of the multidimensional precipitation model proposed by Waymire et al. (1984) are estimated using the areal-averaged radar measurements of precipitation of the Global Atlantic Tropical Experiment (GATE) data set. The procedure followed was the fitting of the first- and second-order moments at different aggregation scales by nonlinear regression techniques. The numerical estimates of the parameters using different subsets of GATE information were reasonably stable, i.e., they were not affected by changes of the area-averaging size, temporal length of the records, and percentage of areal coverage of rainfall. This suggests that the estimation procedure is relatively robust and suitable to estimate the parameters of the multidimensional model in areas of sparse density of rain gages. The use of the space-time spectrum of rainfall to help in the determination of sampling errors due to intermittent visits of future space-borne low-altitude sensors of precipitation is also discussed.

1. INTRODUCTION

Hydrologic models of precipitation have improved significantly in the last decade, evolving from relatively simple models of point precipitation to models which represent the time-dependent two-dimensional rainfall field. Some of these models include those of *Bras and Rodriguez-Iturbe* [1976], *Bell* [1987], *Bell et al.* [this issue], and the WGR model, which is used in the present paper [Waymire et al., 1984; Waymire and Gupta, 1981]. All of these models are stochastic, requiring data from rain gages or radars for tuning their inherent parameters.

At the same time there are several proposals pending to measure precipitation from space, especially over the vast, mostly oceanic tropical band equatorward of latitudes $\pm 35^\circ$ [Simpson, 1988; Simpson et al., 1988]. These and other schemes under discussion use radars and passive microwave radiometers looking down from a low Earth-orbiting platform to measure precipitation. The rain field models mentioned above should play a significant role in the space missions to recover and map fine-scale rainfall over global dimensions. First, the rain field models could help in the planning of missions to check sampling errors due to space-time gaps between visits [e.g., Bell, 1987; Bell et al., 1989; Shin and North, 1988]. Rain field models might also play a role in assessing other errors such as those due to nonhomogeneous fields of view for the sensors [e.g., Chiu et al., 1989; Short and North, this issue]. Finally, one might use the space-derived data once the mission is operational to tune the models for special conditions, inaccessible regions, or over different seasons. In this way the models might actually be brought into near real-time operational use for such applications as flood forecasting and hydroelectric planning as well as for agricultural applications.

In this paper, we wish to approach the possibility of tuning

hydrologic precipitation models with space-derived data. This differs from previous attempts to tune the models, since the space-derived data consist of area averages over sensor fields of view of dimension ranging from 4 km up to about 50 km, depending upon the sensor and satellite configuration being considered. Although some satellite data do exist at present which could be used [e.g., Short and North, this issue], we have chosen to test the idea with a mock data set taken from carefully calibrated surface-based radars taken over the Intertropical Convergence Zone (ITCZ) region of the Atlantic Ocean in 1974, the Global Atmospheric Research Program Atlantic Tropical Experiment (GATE) data set. These rain rate data have been conveniently binned into 4 by 4 km squares, allowing us to aggregate them into larger squares as desired, imitating various satellite detection systems.

We illustrate with the GATE data that the WGR model can be tuned (model parameters successfully estimated) in a way that is reasonably straightforward and robust. Furthermore, the procedure does not largely depend upon the size of the averaging footprint of the data. Our first approach then seems to indicate that the process can be applied to data derived from actual satellite data.

2. THE MULTIDIMENSIONAL PRECIPITATION MODEL

2.1. Introduction

Waymire et al. [1984] developed a mesoscale stochastic precipitation model that incorporates many of the physical features of atmospheric dynamics such as rainbands and cell clustering both in space and time. The WGR model represents precipitation in a hierarchical approach, with rain cells varying in space and in time embedded in so-called cluster potential centers, which in turn are embedded within the rainbands. Although keeping a semblance of reality, the stochastic distributions of all the components were selected to be at the same time mathematically tractable. They derived the first- and second-order moments of the precipitation process $\xi(x, t)$, which represents the rainfall intensity on the ground at time t and spatial coordinates x with units (LT^{-1}). In this paper, only some of the assumptions made in the WGR model are presented. The reader is referred to the original paper for a thorough explanation. Based on those

¹Civil Engineering Department and Climate System Research Program, Texas A&M University, College Station.

²Climate System Research Program, Texas A&M University, College Station.

³Mathematics Department and Climate System Research Program, Texas A&M University, College Station.

Copyright 1990 by the American Geophysical Union.

Paper number 89JD01630.
0148-0227/90/89JD-01630\$05.00

assumptions, *Waymire et al.* [1984] derived the mean and covariance of the point rainfall intensity process $\xi(x, t)$

$$E[\xi(t, x)] = \frac{E[\nu]\rho_L\lambda_m E[i_0]2\pi D^2}{\alpha} \quad (1)$$

$$\begin{aligned} \text{Cov} [\xi(x, t), \xi(t', x')] &= \theta_1 e^{-\alpha|t-t'|} \\ &\cdot \exp\left(-\frac{1}{4D^2} \{[x-x'-u_1(t-t')]^2 + [y-y'-u_2(t-t')]^2\}\right) \\ &+ \theta_2(\beta e^{-\alpha|t-t'|} - \alpha e^{t-t'}) + \theta_3\eta[x-u_1(t-t'), \sigma_1](x') \\ &\cdot \eta[y-u_2(t-t'), \sigma_2](y')(\beta e^{-\alpha|t-t'|} - \alpha e^{-\beta|t-t'|}) \end{aligned} \quad (2)$$

where

$$\begin{aligned} \eta(a, \sigma)(x) &= 1/2\sqrt{\pi(D^2+\sigma^2)} \exp[-(x-a)^2/(4D^2+4\sigma^2)] \\ \theta_1 &= \frac{E[\nu]\rho_L\lambda_m E[i_0^2]\pi D^2}{2\alpha} \\ \theta_2 &= \frac{2\lambda_m\beta E[i_0^2]E^2[\nu]\rho_L^2\pi^2 D^4}{\alpha(\beta^2 - \alpha^2)} \\ \theta_3 &= \frac{2\lambda_m\beta E[i_0^2]E^2[\nu]\rho_L\pi^2 D^4}{\alpha(\beta^2 - \alpha^2)} \end{aligned} \quad (3)$$

where λ_m^{-1} is the average time between storms (in hours), ρ_L is the average number of cluster potential centers (CPCs) in a rainband per unit area (km^{-2}), σ is the cluster spread factor (km), β is the cellular birth rate (hours^{-1}), $E[\nu]$ is the average number of cells per CPC, $\mathbf{u} = (u_1, u_2)$ is the vector of average storm velocities (km h^{-1}), α is the attenuation coefficient in time (hours^{-1}), and D is the attenuation coefficient in space (km).

In passing, we present for future reference an analytical expression for the space-time spectrum $S(\nu_1, \nu_2, f)$ of the instantaneous point rainfall intensity $\xi(x, t)$ derived in our work:

$$\begin{aligned} S(\nu_1, \nu_2, f) &= \theta_1 \frac{\alpha E(D, 0)}{\alpha^2 + 14\pi^2\Theta^2} \\ &+ \left[\theta_2 + \frac{\theta_3}{4\pi(D^2 + \sigma^2)} \right] \alpha\beta E(D, \sigma) \\ &\cdot \left[\frac{1}{\alpha^2 + 14\pi^2\Theta} - \frac{1}{\beta^2 + 14\pi^2\Theta} \right] \end{aligned} \quad (4)$$

where

$$\begin{aligned} E(D, \sigma) &= 8\pi D^2 + \sigma^2 \exp[-4\pi^2(D^2 + \sigma^2)(\nu_1^2 + \nu_2^2)] \\ \Theta &= \nu_1 u_1 + \nu_2 u_2 + f \end{aligned}$$

where ν_1 and ν_2 are the spatial wave numbers and f is the temporal frequency. This analytical form of the space-time spectrum is of interest, since it can be applied in the numerical evaluation of the sampling errors for various measurement designs such as space-borne sensors (G. R. North and S. Nakamoto, Formalism for comparing rain estimation designs, submitted to *Journal of Atmospheric and*

TABLE 1. Typical Numerical Values of the Parameters of the WGR Model

Multi-dimensional Model Parameter	Definition	Unit of Measure	Value
ρ_L	mean density of cluster potentials	10^{-3} cluster/ km^2	4.0
$E[\nu]$	mean number of cells per cluster		8.0
β	cellular birth rate	h^{-1}	1.2
σ	cell location parameter	km	5.0
α	parameter as a measure of mean cell age	h^{-1}	2.0
D	parameter as a measure of spatial extent of cell intensity	km	3.0
λ_m	mean rain band arrival	h^{-1}	0.02
$E[i_0]$	rain cell intensity at cell center at time of birth	mm/h	60.0
u	rain band speed relative to ground	km h^{-1}	30.0

From *Waymire et al.* [1984] and *Valdés et al.* [1985].

Oceanic Technology, 1988; hereinafter referred to as submitted, 1989).

2.2. Parameter Estimation

The WGR model, as presented in the previous equations (1) and (2), has nine parameters, assuming that the velocity vector $\mathbf{u} = (u, 0)$ has a single nonzero velocity element. All of the parameters have to be assigned numerical values before the model is used for simulations. Even though the originators have given nominal values for those parameters and later authors have also provided ranges of some of the parameters (see Table 1 for some of these nominal values), the evaluation of these parameters for a particular site is not an easy task. Extensive analysis of radar information can provide some values, but in many cases of interest, radar data are not available. *Valdés et al.* [1985] developed a simulation model based on the WGR model and addressed the parameter estimation problem using the first- and second-order moments of simulated rainfall as measured in rain gages. They also estimated, by an optimization algorithm, the parameters of the multidimensional process. The results were not totally satisfactory, since the first- and second-order moments of the instantaneous rainfall intensity process were used, which proved to be very unstable.

Recently, *Islam et al.* [1988], based on the previous ideas of *Valdés et al.* [1985], used historical rain gage information at the Walnut Gulch basin in Arizona and successfully derived a procedure to estimate the parameters of the process. They derived the first- and second-order moments of the time-aggregated process, $h_T(x, t)$, aggregated over a time interval T (1 hour, 6 hours, etc.), and used the method of moments to estimate the parameters of the rainfall process. They obtained very satisfactory results. Walnut Gulch has a dense network of rain gages. *Koepsell et al.* [1988] applied the same approach to estimate the parameters in the more common case of a sparse network of rain gages in Brazos County (Texas). The results, although still of a preliminary nature, suggest that the estimates are not as stable as in the Walnut Gulch data, but still satisfactory. The

storms used in the above analysis were classified on a meteorological basis to further explore the capabilities of the estimation approach.

2.3. Parameter Estimation Using Areal-Averaged Measurements

The method due to *Islam et al.* [1988] yields good estimates of the WGR model parameters, provided that rain gage information is available. In some cases, particularly in developing countries, this kind of information may not be readily available. An economic alternative, in the future, will be to obtain this information by space-borne instruments like the ones in the Tropical Rainfall Measurement Mission (TRMM) and Tropical Rainfall Mapping Radar (TRAMAR), which are proposed missions to be launched in the 1990s. Obviously, in the development of this paper, the measurements from these future missions were not available, but an alternative approach was to use the measurements obtained in the GATE experiment, pretending that they came from a space-borne sensor. This idea has been adopted by others in the past [e.g., *McConnell and North*, 1987; *Short and North*, this issue].

In this paper we propose the use of space-borne radar measurements, assuming that spatial averages of the GATE measurements were taken by a space-borne sensor, to estimate the parameters of the WGR model. The procedure employed here is similar to the one proposed by *Islam et al.* [1988], but the aggregation will be done in space and not in time. After the first- and second-order moments of the spatially averaged process instantaneous rainfall intensity at time t , $g(t)$, are evaluated, they will be used by means of a statistical optimization procedure to estimate the parameters of the WGR model.

The analytical first- and second-order moments of the instantaneous areal average intensity, $g(t)$, over a square area L^2 were derived in our work (see the appendix) as follows.

Expected value

$$E[g(t)] = E[\xi(\mathbf{x}, t)] \equiv \bar{\xi} \quad (5)$$

Variance

$$\text{Var}[g(t)] = \frac{1}{L^4} \cdot \left[\theta_1 P^2(D, 0) + (\beta - \alpha) \left(\theta_2 + \frac{\theta_3}{4\pi(D^2 + \sigma^2)} \right) P^2(D, \sigma) \right] \quad (6)$$

where

$$P(D, \sigma) = 4(D^2 + \sigma^2) \left[\exp \left(-\frac{L^2}{4(D^2 + \sigma^2)} \right) - 1 \right] + 2L\sqrt{D^2 + \sigma^2} \sqrt{\pi} \operatorname{erf} \left(\frac{L}{2(D^2 + \sigma^2)^{1/2}} \right)$$

Covariance

$$\text{Cov}[g(t), g(t')] = \frac{1}{L^4} \left[\theta_1 e^{-\alpha|t'|} I_1 I_2 \right.$$

$$\left. + (\beta e^{-\alpha|t'|} - \alpha^{-\beta|t'|}) \left(\theta_2 + \frac{\theta_3}{4\pi(D^2 + \sigma^2)} \right) I_3 I_4 \right] \quad (7)$$

where

$$\begin{aligned} I_1 &= 2D^2[E(L, -u_1, D, 0) \\ &\quad - 2E(0, u_1, D, 0) + E(L, u_1, D, 0)] \\ &\quad + D\sqrt{\pi}[(L - u_1\tau)R(L, -u_1, D, 0) - 2R(0, u_1, D, 0) \\ &\quad + (L + u_1\tau)R(L, u_1, D, 0)] \\ I_2 &= 2D^2[E(L, -u_2, D, 0) \\ &\quad - 2E(0, u_2, D, 0) + E(L, u_2, D, 0)] \\ &\quad + D\sqrt{\pi}[(L - u_2\tau)R(L, u_2, D, 0) \\ &\quad - 2R(0, u_2, D, 0) + (L - u_2\tau)R(L, u_1, D, 0)] \\ I_3 &= 2(D^2 + \sigma^2)[E(L, u_1, D, \sigma) \\ &\quad - 2E(0, u_1, D, \sigma) + E(L, u_1, D, \sigma)] \\ &\quad + [(D^2 + \sigma^2)\pi]^{1/2}[(L - u_1\tau)R(L, -u_1, D, \sigma) \\ &\quad - 2R(0, u_1, D, \sigma) + (L + u_1\tau)R(L, u_1, D, \sigma)] \\ I_4 &= 2(D^2 + \sigma^2)[E(L, -u_1, D, \sigma) \\ &\quad - 2E(0, u_1, D, \sigma) + E(L, u_1, D, \sigma)] \\ &\quad + D\sqrt{\pi}[(L - u_1\tau)R(L, -u_1, D, \sigma) - 2R(0, u_1, D, \sigma) \\ &\quad + (L + u_1\tau)R(L, u_1, D, \sigma)] \\ E(L, u_i, D, \sigma) &= \exp\{- (L - u_i\tau)^2 / [4(D^2 + \sigma^2)]\} \\ R(L, u_i, D, \sigma) &= \operatorname{erf} \left[\frac{L + u_i\tau}{2(D^2 + \sigma^2)^{1/2}} \right] \end{aligned}$$

Details of the derivation of the above equations are given in the appendix. The procedure to be followed is, first, to estimate independently, based upon meteorological analysis of the area under study, three of the multidimensional model parameters: D (attenuation factor in space, km), σ (cluster spread factor in space, km), and u (scalar of average rain-band velocity, km h⁻¹). This approach greatly simplifies the analysis. The remaining six parameters: α , β , ρ_l , $E[v]$, i_0 , and λ_m are unknowns, and they are coupled with six first- and second-order statistics obtained from the areal averages of the rainfall process, forming a nonlinear system of six equations with six unknowns. In an approach similar to that suggested by *Islam et al.* [1988], a relatively rough search technique was used in conjunction with a nonlinear quasi-Newton optimization procedure to produce estimates of the remaining six parameters. The procedure used was the Davidon-Fletcher-Powell technique [e.g., *Luenberger*, 1984], and the scalar objective function was to minimize the sum of the squares of the normalized deviations, i.e.,

$$\min z = \sum_{i=1}^6 [f_i(\mathbf{p})/\theta_i]^2 \quad (8)$$

where $f_i(\mathbf{p})$ is the least squares estimator of θ_i , the i th sample estimate of the second-order statistics, and \mathbf{p} is the vector of

unknown model parameters. This procedure may be carried out for several combinations of spatial aggregation level statistics, e.g., 4×4 and 8×8 km boxes, to evaluate the stability of the estimated parameters of the multidimensional model.

In summary, the steps to follow in the estimation of the parameters of the WGR model using satellite measurements are as follows.

1. Estimate from the areal average measurements the first- and second-order moments of the spatial-averaged instantaneous precipitation process, $g(t)$.

2. Use (5), (6), and (7) to develop a system of nonlinear equations with the parameters of the WGR model as unknowns.

3. By means of a nonlinear optimization procedure (e.g., Davidon-Fletcher-Powell), estimate the unknown coefficients.

This procedure may be carried out using, as an example, the mean, variance, lag-1 autocorrelation coefficient, and several cross correlations for different distances for a given spatial aggregation level (e.g., a 4×4 km box). Then at another spatial aggregation level (e.g., a 16×16 km box), additional equations may be derived to encompass the number of parameters to be estimated.

2.4. Sensitivity Analysis

The estimation procedure is based on the space-time covariance function on the areal average precipitation process. Thus it is important to carry out a sensitivity analysis of the covariance function with regard to particular values of the parameters and the spatial aggregation levels. In particular, as may be seen from (7), the autocovariance function is the statistical moment where all the unknown parameters play a role. To carry out this analysis, and following the ideas of *Islam et al.* [1988], the first-order derivatives of the space-time covariance function as a function of the multidimensional model parameters were analytically evaluated and are shown in section 3 of the appendix. As examples of the sensitivity analysis, the first derivative of the lag-1 autocovariance function of $g(t)$, $\bar{\gamma}(0, 1)$ with regard to the multidimensional model parameters was carried out by varying one parameter over its plausible range and keeping all the

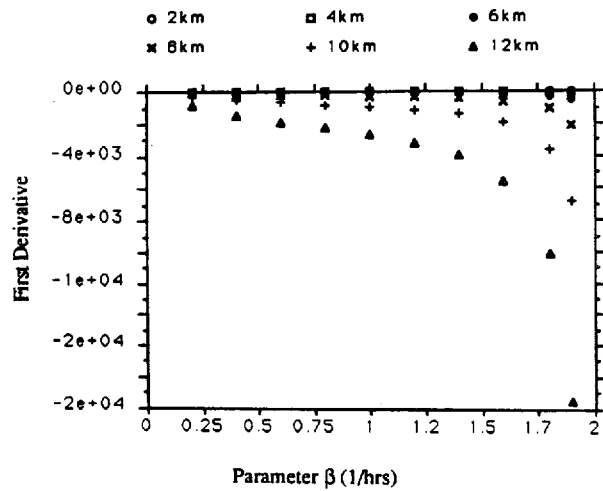


Fig. 1b. Sensitivity analysis of $\bar{\gamma}(0, 1)$ on the parameter β .

others fixed to a particular value as given in Table 1. Illustrative results, from the sensitivity analysis of three of the multidimensional model parameters, α , β , and ρ_L are shown in Figures 1a-1c.

As may be seen from Figure 1a, the first derivative of $\bar{\gamma}(0, 1)$ is relatively insensitive to the most likely values of α for up to 10×10 km area sizes, but it changes for larger-area values, in particular, for a box size of 12×12 km. This is particularly true in the range of values found in the estimation from GATE records. The sensitivity of $\bar{\gamma}(0, 1)$ with regard to parameter β , as shown in Figure 1b, indicates that in the most likely range of this parameter, only 12×12 km boxes show relatively larger variations in the first derivative but still within the same order of magnitude, except at the very end of the range of values of β . We attribute this to the proximity of β to the cell age parameter α , which is prescribed in the Waymire et al. paper, that α^{-1} has to be smaller than β^{-1} . This is consistent with the findings of *Islam et al.* [1988] for temporal aggregation. Again for the range of values found from GATE records the first derivative of the lag-1 autocorrelation function is relatively flat.

Finally, in the analysis of parameter ρ_L , it may be seen that it is the most influenced by size of the area, in particular, at the 10×10 and 12×12 km grid box sizes, and in this case,

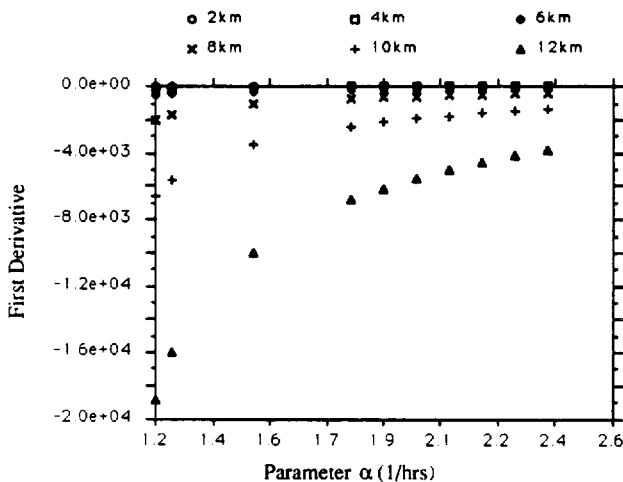


Fig. 1a. Sensitivity analysis of $\bar{\gamma}(0, 1)$ on the parameter α .

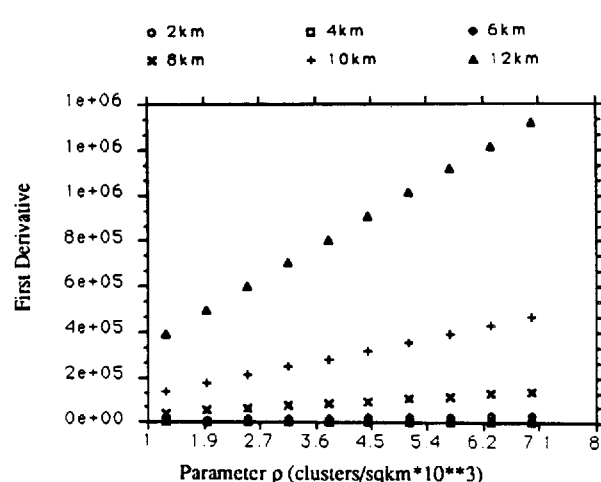


Fig. 1c. Sensitivity analysis of $\bar{\gamma}(0, 1)$ on the parameter ρ_L .

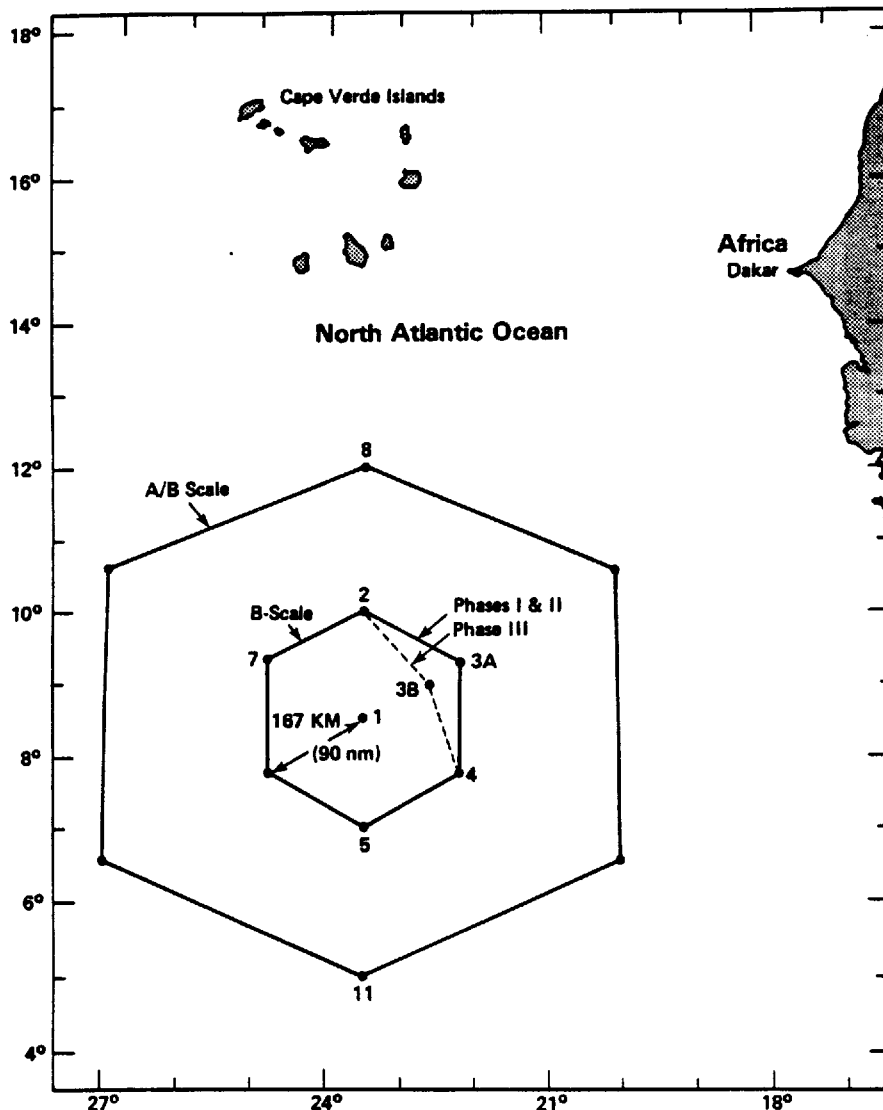


Fig. 2. GATE radar locations within the B- and A/B scale arrays [from Arkell and Hudlow, 1977].

the first derivative is not flat in the neighborhood of the GATE subset estimations carried out in the next section. Similar results were found in the sensitivity analysis of the remaining parameters of the model.

3. APPLICATIONS TO TROPICAL OCEANIC RAINFALL

3.1. Introduction

The procedure for the estimation of the parameters of the WGR model from space-borne sensors measurements was tested by using a subset of well-known radar measurements, the GATE data set. This was done because GATE records are one of the most comprehensive data sets available, even though they were obtained by ship-based radars. The GATE phase I data extend over the period June 28 to July 16, 1974, and provide insight into the tropical processes of the ITCZ.

During the GATE experiment, detailed measurements from rain gages and radar installed on an array of research vessels were made over an area called the B-scale covering a 400-km-diameter hexagon and centered on 8°30'N latitude and 23°30'W longitude off the west coast of Africa (see

Figure 2). Arkell and Hudlow [1977] composited the radar measurements from ships and presented an atlas of radar echos every 15 min. Patterson *et al.* [1979] converted the radar measurements to instantaneous rain rates averaged over 4×4 km pixels.

We did not analyze the whole set of records of GATE, limiting ourselves to a smaller areal and time size subset of the phase I records. In this phase we found missing observations several times. The procedure that we followed was to interpolate if the time interval among existing observations was less than 25 min. If the interval was larger, we discarded that portion of the data set. Thus we had nine sets of observations sampled every 15 min from the original phase I B-scale data set with a spatial resolution of 4×4 km. In the final analysis, we selected a period with 71 observations ("snapshots"), another period with 259 observations, and finally, one with 408 snapshots. Within those data sets, we sampled different area sizes of 104×104 and 128×128 km. The characteristics of the different data sets that were used in the final analysis are given in Tables 2 and 3. From the tables it may be observed that the areal coverage of

TABLE 2. Main Characteristics of GATE Phase I Data Subsets Used in This Study

Data Set	Starting Date	Snapshots	Area, km	Rain Areal Coverage, % of Total Area
I	June 28, 1974	71	104 × 104	19.9
II	June 28, 1974	71	104 × 104	8.7
III	July 5, 1974	251	104 × 104	13.2
IV	June 28, 1974	71	128 × 128	13.4

Sampling interval is 15 min.

oceanic rainfall varies significantly from the value found when the whole GATE data set is analyzed, which was approximately 12% [Simpson, 1988; Chiu, 1988]. It may also be observed from Table 3 that larger variations exist for the first- and second-order moments of the areal-averaged rainfall intensity process, e.g., the mean for set III is 0.1356, and it is 10 times that amount for set I. Similar comments may be made for the other moments of the rainfall process. These large variations are going to make the estimation procedure more difficult, as will be discussed next.

3.2. Applications to GATE Data

The estimation procedure, as outlined in the previous section, was used to evaluate the parameters of the WGR model with very satisfactory results. The results for nine possible combinations of area sizes are given in Tables 4 and 5. As mentioned before, some of the parameters of the model were preassigned based upon experience with GATE data [e.g., Simpson, 1988]. For example, the spatial extent of a rain cell was taken to be of the order of 3–8 km. From this information a numerical value of D equal to 3.0 km was assigned. The cluster spread parameter σ was assumed to be 10.0 km, and the average rainband velocity, u , was taken to be 10.0 km h⁻¹.

The estimated parameters are relatively close, i.e., within the same order of magnitude, as seen in Table 4. During the estimation procedure, smaller values of the sum of squares were obtained when a different value of σ was used for some subsets. In the final table, however, only the results with the same values for the three variables D , σ , and u are reported. From Table 5, where a comparison of the first- and second-order moments is made, it may be observed that the moments are preserved at almost all aggregation levels. In this table, not only the moments used in the estimation are shown, but rather all moments that were available from our analysis of the GATE phase I subsets. The only problem, in our opinion, is the representation of the lag-0 cross correlation, at larger spatial aggregation levels, where the WGR model parameters give smaller correlation values as compared with those observed from the historic records. It was mentioned in our previous work [Valdés et al., 1988] that the autocorrelation times for the multidimensional model, using a hypothetical climate parameter set, stabilized faster than the autocorrelation times of both phases of GATE records. Using better estimates of the multidimensional model parameters, as provided by the estimation procedure, gives closer estimates to the autocorrelation times but still makes the model autocorrelation times go to equilibrium before those of GATE. One possible explanation of this behavior is the

assumption in the WGR model that the cell spatial spread within a cluster follows a bivariate Gaussian distribution, i.e., they have an exponential decay in space. One possible solution to this problem is to use the full description of the bivariate normal by assuming different values of the variances and to use a correlation coefficient to make the spatial distribution function nonsymmetric. The price to pay for this approach is the increase of the number of model parameters from nine to 11.

As may be seen from the tables, the estimation procedure yielded reasonably stable estimates of the multidimensional model parameters. Of particular importance is the result that the parameter estimates using larger areal-average sizes, i.e., simulation run 7 (8 × 8 and 32 × 32 km grid boxes) produced numerical values of the multidimensional model parameters similar to those evaluated from moments of smaller areal-average sizes. Thus it does not seem necessary to obtain areal estimates of rainfall at relatively small areal pixels, at least for the particular purpose of evaluating the parameters of the multidimensional model. In other words, the estimation procedure is relatively insensitive to the size of the averaging footprint of the data, and this has important implications when satellite data become available.

4. FINAL COMMENTS

The results reported in this paper are part of ongoing research at Texas A&M University to characterize tropical rainfall and its application to the planning of future satellite missions. A procedure for the estimation of the parameters of a multidimensional precipitation model, the WGR model, is proposed in this paper.

The estimation procedure uses areal averages of instantaneous rainfall measured by radar. A subset of GATE records is employed to obtain these numerical estimates with satisfactory results. Although, in theory, these results only apply to oceanic tropical rainfall, since the GATE records measured this particular phenomenon, it is our belief that the estimation procedure may be applied to other types of precipitation. We are presently looking to radar measurements of precipitation over land gathered during the Florida

TABLE 3. Areal-Averaged GATE Phase I Subset Rainfall Statistics

Statistic	Data Set			
	I	II	III	IV
Mean, mm/h	1.1841	0.3411	0.1356	1.0999
Variance, 4 × 4 km	25.8050	5.4037	2.6679	26.2184
Lag-1 corr. 4 × 4 km	0.5860	0.3830	0.3910	0.5480
Variance, 8 × 8 km	19.1583	4.4101	2.2121	19.5991
Lag-1 corr. 8 × 8 km	0.7160	0.5510	0.5620	0.6780
Variance, 16 × 16 km				14.5604
Lag-1 corr. 16 × 16 km				0.8250
Variance, 32 × 32 km				11.5664
Lag-1 corr. 32 × 32 km				0.9050
Lag-zero cross				
4 × 4 km	0.3540	0.3860	0.3550	0.3680
8 × 8 km	0.2850	0.2910	0.2260	0.2880
16 × 16 km				0.1910
32 × 32 km				0.1010

All lag-zero cross correlations were computed at a distance equal to the length of the box size on the x axis, measured from edge to edge.

TABLE 4. Multidimensional Model Parameter Estimation Results

Run No.	Spatial Aggregation, km				Parameter						Data Set	Sum of Squares
	4 × 4	8 × 8	16 × 16	32 × 32	λ, bands/h	β, cells/h	E[ν], cells/cluster	α, 1/h	ρ, cluster/km ²	E[io], mm/h		
1	μ, σ ₂ , ρ ₁ , ρ ₀	σ ₂ , ρ ₁			0.0168	0.1991	3.04	1.34	0.00867	63.95	I	0.1109
2	μ, σ ₂ , ρ ₁ , ρ ₀	σ ₂ , ρ ₁			0.0128	0.3552	3.82	1.73	0.00383	55.06	II	0.0207
3	μ, σ ₂ , ρ ₁ , ρ ₀	σ ₂ , ρ ₁			0.0111	0.6818	4.60	1.78	0.00215	46.17	III	0.1260
4	μ, σ ₂ , ρ ₁ , ρ ₀		σ ₂ , ρ ₁		0.0146	0.1849	9.44	1.32	0.00244	77.77	IV	0.0632
5	μ, σ ₂ , ρ ₁ , ρ ₀		σ ₂ , ρ ₁	σ ₂ , ρ ₁	0.0131	0.2275	8.66	1.32	0.00294	78.77	IV	0.1794
6		μ, σ ₂ , ρ ₁ , ρ ₀	σ ₂ , ρ ₁		0.0235	0.4688	5.38	1.33	0.00383	55.06	IV	0.0229
7		μ, σ ₂ , ρ ₁ , ρ ₀		σ ₂ , ρ ₁	0.0235	0.63919	3.30	1.32	0.00600	57.04	IV	0.1155
8	μ, σ ₂ , ρ ₁ , ρ ₀	σ ₂ , ρ ₂			0.0168	0.2274	3.04	1.32	0.00837	63.95	IV	0.0705
9			μ, σ ₂ , ρ ₁ , ρ ₀	σ ₂ , ρ ₁	0.0167	0.6817	7.62	1.33	0.00985	20.49	IV	0.1419

Here, μ, areal-averaged instantaneous mean; σ₂, areal-averaged variance; ρ₁, lag-1 autocorrelation; and ρ₀, lag-zero cross correlation.

Area Cumulus Experiment (FACE) to perform a similar analysis.

We acknowledge the fact that the results reported in this paper are related to a small subset of GATE and some further analysis may be required. However, it is our feeling that the subset actually reproduced most of the characteristics previously reported for the entire GATE data set. Since radar measurements like the ones obtained in GATE may be used to simulate space-borne measurements, we believe that the WGR model and the precipitation information obtained from space-borne sensors in future planned missions will complement each other. Remote sensing of tropical precipitation will cover areas of sparse density of rain gages and should result in a better estimation of the parameters of the

WGR model. This will greatly increase the applicability of this multidimensional model to the field of hydrology.

The space-time spectrum for instantaneous point precipitation intensity that was analytically derived from the multidimensional model equations may be used in several ways. One is to further analyze the capability of the WGR model to represent tropical oceanic rainfall. This can be done by comparing spectra for data and model. For a study of GATE space-time spectra the reader is referred to S. Nakamoto et al. (Frequency wave number spectrum for the GATE phase I rainfield, submitted to *Journal of Applied Meteorology*, 1989). Another application is to the analytical estimation of the sampling errors for various measurement designs by spectral methods (G. R. North and S. Nakamoto, submitted

TABLE 5. Comparison of Estimated and Historic Moments of GATE Phase I Subsets

Run No.	Means		Moment	Spatial Aggregation, km							
	Data	Estimated		4 × 4		8 × 8		16 × 16		32 × 32	
				Data	Estimated	Data	Estimated	Data	Estimated	Data	Estimated
1	1.1732	1.2106	Variance	26.8050	24.9025	19.1583	19.6678				
			Lag-1 autocorr.	0.5680	0.4897	0.7160	0.5710				
			Lag-zero crosscorr.	0.3540	0.4252	0.2850	0.2329				
2	0.3411	0.3372	Variance	5.4037	5.5673	4.4101	4.3264				
			Lag-1 autocorr.	0.3830	0.4128	0.5510	0.4882				
			Lag-zero crosscorr.	0.3860	0.3932	0.2910	0.2023				
3	0.1356	0.1610	Variance	2.6679	2.3764	2.2121	1.8742				
			Lag-1 autocorr.	0.3910	0.4246	0.5620	0.4976				
			Lag-zero crosscorr.	0.3550	0.4223	0.2260	0.2302				
4	1.0999	1.1175	Variance	26.2184	27.7957	19.5991	21.9246	14.5604	13.4863	11.5664	6.8161
			Lag-1 autocorr.	0.5480	0.4878	0.6780	0.5691	0.8250	0.7091	0.9050	0.8151
			Lag-zero crosscorr.	0.3680	0.4226	0.2880	0.2304	0.1910	0.0787	0.1010	0.0028
5	1.0999	1.1213	Variance	26.2184	30.6798	19.5991	24.6275	14.5604	15.7552	11.5664	8.2634
			Lag-1 autocorr.	0.5480	0.5204	0.6780	0.6007	0.8250	0.7349	0.9050	0.8325
			Lag-zero crosscorr.	0.3680	0.4578	0.2880	0.2630	0.1910	0.0868	0.1010	0.0030
6	1.0999	1.1361	Variance	26.2184	24.7887	19.5991	20.3933	14.5604	13.7387	11.5664	7.5319
			Lag-1 autocorr.	0.5480	0.5571	0.6780	0.6324	0.8250	0.7518	0.9050	0.8342
			Lag-zero crosscorr.	0.3680	0.5081	0.2880	0.3076	0.1910	0.8342	0.1010	0.0032
7	1.0999	1.1333	Variance	26.2184	27.1114	19.5991	22.5164	14.5604	15.4584	11.5664	8.6048
			Lag-1 autocorr.	0.5480	0.5669	0.6780	0.6391	0.8250	0.7510	0.9050	0.8265
			Lag-zero crosscorr.	0.3680	0.5278	0.2880	0.3245	0.1910	0.1006	0.1010	0.0032
8	1.0999	1.1692	Variance	26.2184	24.7526	19.5991	19.6459	14.5604	12.2878	11.5664	6.3104
			Lag-1 autocorr.	0.5480	0.5003	0.6780	0.5812	0.8250	0.7185	0.9050	0.8206
			Lag-zero crosscorr.	0.3680	0.4372	0.2880	0.2441	0.1910	0.0822	0.1010	0.0029
9	1.0999	1.1047	Variance	26.2184	22.2684	19.5991	20.2053	14.5604	16.1811	11.5664	10.0262
			Lag-1 autocorr.	0.5480	0.7386	0.6780	0.7788	0.8250	0.8330	0.9050	0.8708
			Lag-zero crosscorr.	0.3680	0.7214	0.2880	0.4750	0.1910	0.1276	0.1010	0.0037

1989). Of special interest is the case of a low orbiting satellite which makes visits at fixed intervals. The WGR space-time spectrum presented in this paper provides another example for which the spectral method can be applied.

If the WGR model is to be used to represent multidimensional precipitation traces for simulation of future satellite missions, it must account for the fact that the space-borne sensor will cover partially only the area under study (grid box) during each visit. The effect of this on the sampling errors should then be analyzed. To approach this problem, Bell [1987], Bell *et al.* [this issue], and Shin and North [1988] took calculated satellite orbits to determine the fraction of the grid box covered in each pass. In our earlier work [Valdés *et al.*, 1988] we made the assumption that the whole area was observed at each visit. In a future study we expect to apply the WGR model to the sampling problem, making use of the true coverage on each overpass as computed from exact satellite orbits.

APPENDIX

Introduction

For the point rainfall intensity process $\xi(\mathbf{x}, t)$ Waymire *et al.* [1984] derived the expected value $E[\xi(\mathbf{x}, t)]$, the variance $\text{Var}[\xi(\mathbf{x}, t)]$, the covariance $\text{Cov}[\xi(\mathbf{x}, t), \xi(\mathbf{x}', t')]$, where $\mathbf{x} = (x_1, x_2)$ and $\mathbf{x}' = (x'_1, x'_2)$.

The areal average of the random variable $\xi(\mathbf{x}, t)$ over a square area L^2 is defined as

$$g(t) = \frac{1}{L^2} \int_0^L dx_1 \int_0^L dx_2 \xi(\mathbf{x}, t) \quad (\text{A1})$$

Since the precipitation process was assumed to be weakly ergodic by Waymire *et al.* [1984], the expected value of $g(t)$ is obtained by performing time averages. Namely, the expected value for $g(t)$ can be computed by

$$E[\xi(L, t)] = \lim_{T \rightarrow \infty} \frac{1}{T} \int_0^T dt g(t) \quad (\text{A2})$$

Since the expected value operator $E[\]$ commutes with the spatial integral operator in (A1), the expected value of the area-averaged rain intensity is not affected by the area-averaging process, i.e., the mean value for the point process is equal to the mean value for the area-averaged rain rate

$$E[g(t)] = E[\xi(\mathbf{x}, t)] \equiv \bar{\xi} \quad (\text{A3})$$

The variance and covariance of $g(t)$ defined as

$$\text{Var}[g(t)] = E\{(g(t) - E[g(t)])^2\} \quad (\text{A4})$$

$$\text{Cov}[g(t), g(t')] = E\{(g(t) - E[g(t)])(g(t') - E[g(t')])\} \quad (\text{A5})$$

must be affected by the area averaging, since the expected value operator $E[\]$ apparently does not commute with the products of the integral operator in the right-hand sides of the above two equations. In practice, smoothing is widely used to filter sequences, in order to diminish the effect of measurement errors and other high-frequency disturbances. We expect that the area-averaging process will reduce the variance of the random variables.

Waymire *et al.* [1984] did not provide an analytical spectrum of the instantaneous point intensity, $\xi(\mathbf{x}, t)$. This is important for the evaluation of sampling errors of precipitation by intermittent visits by space-borne sensors.

Using the Wiener-Khinchin relation [Bras and Rodriguez-Iturbe, 1984], the wave number frequency spectrum for the point process may be computed as

$$S(\nu_1, \nu_2, f) = \int_{-\infty}^{+\infty} d\zeta_1 \int_{-\infty}^{+\infty} d\zeta_2 \cdot \int_{-\infty}^{+\infty} d\tau \text{Cov}[\xi(\mathbf{x}, t), \xi(\mathbf{x}', (t'))] e^{2\pi i(\nu_1 \zeta_1 + \nu_2 \zeta_2 + f\tau)} \quad (\text{A6})$$

where $\zeta_1 = x_1 - x'_1$, $\zeta_2 = x_2 - x'_2$, and $\tau = t_1 - t_2$.

In our application to the GATE data, which have a 4×4 km areal resolution, the space correlation function of 4×4 km area-averaged rain intensity is $g(t)$. Thus the value of $q(\mathbf{x}, t)$ is the area-averaged rain intensity over a square of area l^2 :

$$q(\mathbf{x}, t) = \frac{1}{l^2} \int_{x_1}^{x_1+l} dx_1 \int_{x_2}^{x_2+l} dx_2 \xi(\mathbf{x}, t) \quad (\text{A7})$$

where l is the length of the averaging area, which is specified by its lower left end point of the integration (x_1, x_2) . The space-time covariance for the area-averaged rain intensity is

$$\text{Cov}[q(\mathbf{x}, t), q(\mathbf{x}', t')] = E\{(q(\mathbf{x}, t) - \bar{q})(q(\mathbf{x}', t') - \bar{q})\} \quad (\text{A8})$$

Notice that the above-defined covariance is reduced to the covariance for the area-averaged rain rate in (A6) if $\mathbf{x} = \mathbf{x}' = 0$ and $l = L$. The next section of this appendix is devoted to deriving analytical expressions of the space-time spectrum $S(\nu_1, \nu_2, f)$ and the covariance $\text{Cov}[q(\mathbf{x}, t), q(\mathbf{x}', t')]$.

Covariance and Spectrum

Inserting (A7) into (A8) and using the commutability of the ensemble operator $E[\]$ with the local areal integration over l^2 , the covariance of the local area-averaged rain intensity may be expressed as

$$\begin{aligned} \text{Cov}[q(\mathbf{x}, t), q(\mathbf{x}', t')] &= \frac{1}{l^4} \int_{x_1}^{x_1+l} dy_1 \int_{x_2}^{x_2+l} dy_2 \int_{x'_1}^{x'_1+l} dy_1 \int_{x'_2}^{x'_2+l} dy_2 \\ &\cdot \text{Cov}[\xi(t, y_1, y_2), \xi(t', y'_1, y'_2)] \\ &= \frac{1}{l^4} \left(\int_0^{x_1+l} dy_1 - \int_0^{x_1} dy_1 \right) \\ &\cdot \left(\int_0^{x_2+l} dy_2 - \int_0^{x_2} dy_2 \right) \\ &\cdot \left(\int_0^{x'_1+l} dy'_1 - \int_0^{x'_1} dy'_1 \right) \\ &\cdot \left(\int_0^{x'_2+l} dy'_2 - \int_0^{x'_2} dy'_2 \right) \end{aligned}$$

$$\begin{aligned}
&= \frac{1}{l^4} [I(x_1 + l, x_2 + l, x'_1 + l, x'_2 + l) \\
&\quad - I(x_1 + l, x_2 + l, x'_1 + l, x'_2) \\
&\quad - I(x_1 + l, x_2 + l, x'_1, x'_2 + l) \\
&\quad + I(x_1 + l, x_2 + l, x'_1, x'_2) \\
&\quad - I(x_1 + l, x_2, x'_1 + l, x'_2 + l) \\
&\quad + I(x_1 + l, x_2, x'_1 + l, x'_2) \\
&\quad - I(x_1 + l, x_2, x'_1, x'_2 + l) - I(x_1 + l, x_2, x'_1, x'_2) \\
&\quad - I(x_1, x_2 + l, x'_1, x'_1 + l, x'_2 + l) \\
&\quad + I(x_1, x_2 + l, x'_1 + l, x'_2) \\
&\quad + I(x_1, x_2 + l, x'_1, x'_2 + l) - I(x_1, x_2 + l, x'_1, x'_2) \\
&\quad + I(x_1, x_2, x'_1 + l, x'_2 + l) - I(x_1, x_2, x'_1 + l, x'_2) \\
&\quad - I(x_1, x_2, x'_1, x'_2 + l) + I(x_1, x_2, x'_1, x'_2)] \quad (A9)
\end{aligned}$$

where

$$\begin{aligned}
I(l_1, l_2, l_3, l_4) &= \int_0^{l_1} dy_1 \int_0^{l_2} dy_2 \int_0^{l_3} dy'_1 \int_0^{l_4} dy'_2 \\
&\quad \text{Cov} [\xi(t, y_1, y_2), \xi(t', y'_1, y'_2)] \\
&= \theta_1 e^{-\alpha|\tau|} J(-u_1\tau, 2D, l_1, l_3) J(-u_2\tau, 2D, l_2, l_4) \\
&\quad + \left(\theta_2 + \frac{\theta_3}{4\pi(D^2 + \sigma^2)} \right) [\beta e^{-\alpha|\tau|} - \alpha e^{-\beta|\tau|}] \\
&\quad \cdot J[u_1\tau, 2(D^2 + \sigma^2)^{1/2}, l_3, l_1] \\
&\quad \cdot J[u_2\tau, 2(D^2 + \sigma^2)^{1/2}, l_4, l_2] \quad (A10)
\end{aligned}$$

and

$$\begin{aligned}
J(a, b, l_1, l_2) &= \frac{b\sqrt{\pi}}{2} \left\{ (l_2 - a) \left[\text{erf} \left(\frac{a}{b} \right) \right. \right. \\
&\quad \left. \left. - \text{erf} \left(\frac{a - l_2}{b} \right) \right] + l_2 \left[\text{erf} \left(\frac{l_1 - l_2 + a}{b} \right) - \text{erf} \left(\frac{a}{b} \right) \right] \right. \\
&\quad \left. + (l_1 + a) \left[\text{erf} \left(\frac{l_1 + a}{b} \right) - \text{erf} \left(\frac{l_1 - l_2 + a}{b} \right) \right] \right. \\
&\quad \left. + \frac{b^2}{2} \left[\exp \left[- \left(\frac{a - l_2}{b} \right)^2 \right] - \exp \left[- \left(\frac{a}{b} \right)^2 \right] \right] \right. \\
&\quad \left. + \exp \left[- \left(\frac{a + l_1}{b} \right)^2 \right] \right. \\
&\quad \left. - \exp \left[- \left(\frac{a + l_1 - l_2}{b} \right)^2 \right] \right\} \quad (A11)
\end{aligned}$$

Inserting the covariance for the point process $\text{Cov} [\xi(x, t), \xi(x', (t'))]$, the wave number frequency spectrum for the point process is

$$\begin{aligned}
S(\nu_1, \nu_2, f) &= \theta_1 \int_{-\infty}^{+\infty} d\xi_1 \int_{-\infty}^{+\infty} d\xi_2 \int_{-\infty}^{+\infty} d\tau \\
&\quad \cdot \exp \{-\alpha|\tau| - [(\xi_1 - u_1\tau)^2 + (\xi_2 - u_2\tau)^2] \\
&\quad + 2\pi i(\xi_1\nu_1 + \xi_2\nu_2 + \tau f)\} \\
&\quad + \left(\theta_2 + \frac{\theta_3}{4\pi(D^2 + \sigma^2)} \right) \int_{-\infty}^{+\infty} d\xi_1 \int_{-\infty}^{+\infty} d\xi_2 \int_{-\infty}^{+\infty} d\tau \\
&\quad \cdot (\beta e^{-\alpha|\tau|} - e^{-\beta|\tau|}) \exp \{[(\xi_1 - u_1\tau)^2 + (\xi_2 - u_2\tau)^2] \\
&\quad + 2\pi i(\xi_1\nu_1 + \xi_2\nu_2 + \tau f)\} \quad (A12)
\end{aligned}$$

The integration of the right-hand side is essentially reduced to the estimation of the following integral:

$$\begin{aligned}
K &= \int_{-\infty}^{+\infty} dx_1 \int_{-\infty}^{+\infty} dx_2 \\
&\quad \cdot \exp \left[- \left(\frac{x_1}{2D} - 2\pi D\nu_1 i \right)^2 - 4\pi^2 D^2 \nu_1^2 \right. \\
&\quad \left. - \left(\frac{x_2}{2D} - 2\pi D\nu_2 i \right)^2 - 4\pi^2 D^2 \nu_2^2 \right] \\
&\quad \cdot \left(\int_0^{+\infty} dx_3 \exp [-\alpha x_3 + 2\pi i(\nu_1 u_1 + \nu_2 u_2 + f)x_3] \right) \\
&\quad + \exp [-\alpha x_3 - 2\pi i(\nu_1 u_1 + \nu_2 u_2 + f)x_3] \\
&= \frac{4\alpha\pi D \exp [-4\pi^2 D^2 (\nu_1^2 + \nu_2^2)]}{\alpha^2 + 16\pi^4 (\nu_1 u_1 + \nu_2 u_2 + f)^2} \quad (A13)
\end{aligned}$$

Using the above integration, the wave number frequency spectrum (A12) can be written

$$\begin{aligned}
S(\nu_1, \nu_2, f) &= \theta_1 \frac{\alpha E(D, 0)}{\alpha^2 + 14\pi^2 \Theta^2} + \left(\theta_2 + \frac{\theta_3}{4\pi(D^2 + \sigma^2)} \right) \\
&\quad \cdot \alpha \beta E(D, \sigma) \left(\frac{1}{\alpha^2 + 14\pi^2 \Theta^2} - \frac{1}{\beta^2 + 14\pi^2 \Theta^2} \right) \quad (A14)
\end{aligned}$$

where

$$\begin{aligned}
E(D, \sigma) &= 8\pi(D^2 + \sigma^2) \exp [-4\pi^2(D^2 + \sigma^2)(\nu_1^2 + \nu_2^2)] \\
\Theta &= \nu_1 u_1 + \nu_2 u_2 + f
\end{aligned}$$

Sensitivity Analysis

In this section the theoretical lag-1 autocorrelation coefficient $\rho(0, 1)$ is defined as

$$\rho(0, 1) = \frac{\gamma(0, 1)}{\gamma(0, 0)} \quad (A15)$$

The gradient of $\rho(0, 1)$ with respect to a particular parameter p , keeping all other parameters fixed, will be investigated to illustrate the interplay between the parameters and the autocorrelation function of the rainfall process.

$$\frac{\partial \rho(0, 1)}{\partial p} = \frac{1}{\gamma^2(0, 0)} \left(\frac{\partial \gamma(0, 0)}{\partial p} \gamma(0, 0) - \frac{\partial \gamma(0, 1)}{\partial p} \gamma(0, 1) \right) + H(\beta e^{-\alpha} - \alpha e^{-\beta}) \left(\frac{\partial \theta_2}{\partial \beta} + \frac{\partial T}{\partial \beta} \right) \quad (\text{A16})$$

where p represents the parameters of the multidimensional model: α , β , λ_m , ρ_L , $E[i_0]$, and $E[\nu]$. The lag-1 autocovariance $\gamma(0, 1)$ and covariance $\gamma(0, 0)$ are expressed as

$$\gamma(0, 1) = \frac{1}{l^4} [\theta_1 e^{-\alpha} G + (\beta e^{-\alpha} - \alpha e^{-\beta})(\theta_2 + T)H] \quad (\text{A17})$$

$$\gamma(0, 0) = \frac{1}{l^4} [\theta_1 A + (\beta - \alpha)(\theta_2 + T)B] \quad (\text{A18})$$

where

$$A = J^2(0, 2D, l, l)$$

$$B = J^2(0, 2(D^2 + \sigma^2)^{1/2}, l, l)$$

$$G = J(-u_1, 2D, l, l)J(-u_2, 2D, l, l)$$

$$H = J(u_1, 2(D^2 + \sigma^2)^{1/2}, l, l)J(u_2, 2(D^2 + \sigma^2)^{1/2}, l, l)$$

$$T = \frac{\theta_3}{4\pi(D^2 + \sigma^2)}$$

Notice that θ_i is a function of α , β , λ_m , ρ_L , $E[i_0]$, and $E[\nu]$. The derivatives of the covariance in (A16) are written as

$$\bar{\gamma}(0, 0) = l^4 \gamma(0, 0)$$

$$\frac{\partial \bar{\gamma}(0, 0)}{\partial \alpha} = A \left(\frac{\partial \theta_1}{\partial \alpha} \right) - B(\theta_2 + T) + B(\beta - \alpha) \left(\frac{\partial \theta_2}{\partial \alpha} + \frac{\partial T}{\partial \alpha} \right)$$

$$\frac{\partial \bar{\gamma}(0, 0)}{\partial \beta} = A \left(\frac{\partial \theta_1}{\partial \beta} \right) - B(\theta_2 + T) + B(\beta - \alpha) \left(\frac{\partial \theta_2}{\partial \beta} + \frac{\partial T}{\partial \beta} \right)$$

$$\frac{\partial \bar{\gamma}(0, 0)}{\partial E[i_0]} = A \left(\frac{\partial \theta_1}{\partial E[i_0]} \right) + B(\beta - \alpha) \left(\frac{\partial \theta_2}{\partial E[i_0]} + \frac{\partial T}{\partial E[i_0]} \right)$$

$$\frac{\partial \bar{\gamma}(0, 0)}{\partial E[\nu]} = A \left(\frac{\partial \theta_1}{\partial E[\nu]} \right) + B(\beta - \alpha) \left(\frac{\partial \theta_2}{\partial E[\nu]} + \frac{\partial T}{\partial E[\nu]} \right)$$

$$\frac{\partial \bar{\gamma}(0, 0)}{\partial \lambda_m} = A \left(\frac{\partial \theta_1}{\partial \lambda_m} \right) + B(\beta - \alpha) \left(\frac{\partial \theta_2}{\partial \lambda_m} + \frac{\partial T}{\partial \lambda_m} \right)$$

$$\frac{\partial \bar{\gamma}(0, 0)}{\partial \rho_L} = A \left(\frac{\partial \theta_1}{\partial \rho_L} \right) + B(\beta - \alpha) \left(\frac{\partial \theta_2}{\partial \rho_L} + \frac{\partial T}{\partial \rho_L} \right)$$

Similarly, the derivatives of the lag-1 autocorrelation with regard to the model parameters are

$$\bar{\gamma}(0, 1) = l^4 \gamma(0, 1)$$

$$\begin{aligned} \frac{\partial \bar{\gamma}(0, 1)}{\partial \alpha} = & -G\theta_1 e^{-\alpha} + G \left(\frac{\partial \theta_1}{\partial \alpha} \right) e^{-\alpha} + H(\beta e^{-\alpha} - \alpha e^{-\beta}) \\ & \cdot (\theta_2 + T) + H(\beta e^{-\alpha} - \alpha e^{-\beta}) \left(\frac{\partial \theta_2}{\partial \alpha} + \frac{\partial T}{\partial \alpha} \right) \end{aligned}$$

$$\frac{\partial \bar{\gamma}(0, 1)}{\partial \beta} = +H(e^{-\alpha} + \alpha e^{-\beta})(\theta_2 + T)$$

$$\frac{\partial \bar{\gamma}(0, 1)}{\partial E[i_0]} = +G \left(\frac{\partial \theta_1}{\partial E[i_0]} \right) e^{-\alpha}$$

$$+ H(\beta e^{-\alpha} - \alpha e^{-\beta}) \left(\frac{\partial \theta_2}{\partial E[i_0]} + \frac{\partial T}{\partial E[i_0]} \right)$$

$$\frac{\partial \bar{\gamma}(0, 1)}{\partial E[\nu]} = +G \left(\frac{\partial \theta_1}{\partial E[\nu]} \right) e^{-\alpha}$$

$$+ H(\beta e^{-\alpha} - \alpha e^{-\beta}) \left(\frac{\partial \theta_2}{\partial E[\nu]} + \frac{\partial T}{\partial E[\nu]} \right)$$

$$\frac{\partial \bar{\gamma}(0, 1)}{\partial \lambda_m} = +G \left(\frac{\partial \theta_1}{\partial \lambda_m} \right) e^{-\alpha} + H(\beta e^{-\alpha} - \alpha e^{-\beta}) \left(\frac{\partial \theta_2}{\partial \lambda_m} + \frac{\partial T}{\partial \lambda_m} \right)$$

$$\frac{\partial \bar{\gamma}(0, 1)}{\partial \rho_L} = +G \left(\frac{\partial \theta_1}{\partial \rho_L} \right) e^{-\alpha} + H(\beta e^{-\alpha} - \alpha e^{-\beta}) \left(\frac{\partial \theta_2}{\partial \rho_L} + \frac{\partial T}{\partial \rho_L} \right)$$

The derivatives

$$\frac{\partial \theta_1}{\partial \alpha} = - \frac{E[\nu] \rho_L \lambda_m E[i_0^2] \pi D^2}{2\alpha^2}$$

$$\frac{\partial \theta_1}{\partial \beta} = 0$$

$$\frac{\partial \theta_1}{\partial E[i_0]} = \frac{E[\nu] \rho_L \lambda_m E[i_0] \pi D^2}{2\alpha}$$

$$\frac{\partial \theta_1}{\partial E[\nu]} = \frac{\rho_L \lambda_m E[i_0^2] \pi D^2}{2\alpha}$$

$$\frac{\partial \theta_1}{\partial \lambda_m} = \frac{E[\nu] \rho_L E[i_0^2] \pi D^2}{2\alpha}$$

$$\frac{\partial \theta_1}{\partial \rho_L} = \frac{E[\nu] \lambda_m E[i_0^2] \pi D^2}{2\alpha}$$

$$\frac{\partial \theta_2}{\partial \alpha} = -2 \frac{\beta(\beta - 3\alpha^2)}{\alpha^2(\beta^2 - \alpha^2)^2} \lambda_m E[i_0^2] E[\nu]^2 \rho_L^2 \pi^2 D^4$$

$$\frac{\partial \theta_2}{\partial \beta} = -2 \frac{\beta(\alpha^2 + 2\beta^2)}{\alpha^2(\beta^2 - \alpha^2)^2} \lambda_m E[i_0^2] E[\nu]^2 \rho_L^2 \pi^2 D^4$$

$$\frac{\partial \theta_2}{\partial E[i_0]} = -2 \frac{4\lambda_m \beta E[i_0] E[\nu]^2 \rho_L^2 \pi^2 D^4}{\alpha^2(\beta^2 - \alpha^2)^2}$$

$$\frac{\partial \theta_2}{\partial E[\nu]} = -2 \frac{4\lambda_m \beta E[i_0^2] E[\nu] \rho_L^2 \pi^2 D^4}{\alpha^2(\beta^2 - \alpha^2)^2}$$

$$\frac{\partial \theta_2}{\partial \lambda_m} = -2 \frac{4\beta E[i_0^2] E[\nu]^2 \rho_L^2 \pi^2 D^4}{\alpha^2(\beta^2 - \alpha^2)^2}$$

$$\frac{\partial \theta_2}{\partial \rho_L} = -2 \frac{4\lambda_m \beta E[i_0] E[\nu]^2 \rho_L \pi^2 D^4}{\alpha^2(\beta^2 - \alpha^2)^2}$$

$$\frac{\partial \theta_3}{\partial \alpha} = -2 \frac{\beta(\beta - 3\alpha^2)}{\alpha^2(\beta^2 - \alpha^2)^2} \lambda_m E[i_0^2] E[\nu]^2 \rho_L^2 \pi^2 D^4$$

$$\frac{\partial \theta_3}{\partial \beta} = -2 \frac{\beta(\alpha^2 + 2\beta^2)}{\alpha^2(\beta^2 - \alpha^2)^2} \lambda_m E[i_0^2] E[\nu]^2 \rho_L^2 \pi^2 D^4$$

$$\frac{\partial \theta_3}{\partial E[i_0]} = -2 \frac{4\lambda_m \beta E[i_0] E[\nu]^2 \rho_L^2 \pi^2 D^4}{\alpha^2(\beta^2 - \alpha^2)^2}$$

$$\frac{\partial \theta_3}{\partial E[\nu]} = -2 \frac{4\lambda_m \beta E[i_0^2] E[\nu] \rho_L^2 \pi^2 D^4}{\alpha^2(\beta^2 - \alpha^2)^2}$$

$$\frac{\partial \theta_3}{\partial \lambda_m} = -2 \frac{2\beta E[i_0^2] E[\nu]^2 \rho_L^2 \pi^2 D^4}{\alpha^2(\beta^2 - \alpha^2)^2}$$

$$\frac{\partial \theta_3}{\partial \rho_L} = -2 \frac{2\lambda_m \beta E[i_0^2] E[\nu]^2 \rho_L \pi^2 D^4}{\alpha^2(\beta^2 - \alpha^2)^2}$$

$$\frac{\partial T}{\partial \alpha} = \frac{\partial \theta_3 / \partial \alpha}{4\pi(D^2 + \sigma^2)}$$

$$\frac{\partial T}{\partial \beta} = \frac{\partial \theta_3 / \partial \beta}{4\pi(D^2 + \sigma^2)}$$

$$\frac{\partial T}{\partial E[i_0]} = \frac{\partial \theta_3 / \partial E[i_0]}{4\pi(D^2 + \sigma^2)}$$

$$\frac{\partial T}{\partial E[\nu]} = \frac{\partial \theta_3 / \partial E[\nu]}{4\pi(D^2 + \sigma^2)}$$

$$\frac{\partial T}{\partial \lambda_m} = \frac{\partial \theta_3 / \partial \lambda_m}{4\pi(D^2 + \sigma^2)}$$

$$\frac{\partial T}{\partial \rho_L} = \frac{\partial \theta_3 / \partial \rho_L}{4\pi(D^2 + \sigma^2)}$$

Acknowledgments. This research was partially funded through NASA grant NAS-5-869. K. S. Shin, J.-T. Wang, C. Graves, at the Climate System Research Program (CSRP), and D. A. Short at NASA gave invaluable comments. Phil Riba (CSRP) was greatly helpful with the computational details of this work. S. Islam and R. L. Bras from MIT kindly provided us with their optimization algorithm which was very helpful in developing ours. The comments of two anonymous referees contributed to improvements in the manuscript. All contributions are gratefully acknowledged.

REFERENCES

- Arkell, R., and M. Hudlow, GATE international meteorological radar atlas, U.S. Dep. of Commer., NOAA, Washington, D. C., 222 pp., 1977.
- Bell, T. L., A space-time stochastic model of rainfall for satellite remote-sensing studies, *J. Geophys. Res.*, 92, 9631-9643, 1987.
- Bell, T. L., A. Abdullah, R. L. Martin, and G. R. North, Sampling errors for satellite-derived tropical rainfall: Monte Carlo study using a space-time stochastic model, *J. Geophys. Res.*, this issue.
- Bras, R. L., and I. Rodriguez-Iturbe, Rainfall generation: A nonstationary time-varying multidimensional model, *Water Resour. Res.*, 12(3), 450-456, 1976.
- Bras, R. L., and I. Rodriguez-Iturbe, *Random Functions and Hydrology*, Addison-Wesley, Reading, Mass., 1984.
- Chiu, L. S., Rain estimation from satellites: Areal rainfall-rain area relation, paper presented at the Third Conference on Satellite Meteorology and Oceanography, Am. Meteorol. Soc., Anaheim, Calif., Feb. 1988.
- Chiu, L. S., G. R. North, D. A. Short, and A. McConnell, Rain estimation of satellites: Effect of finite field of view, *J. Geophys. Res.*, this issue.
- Islam, S., R. L. Bras, and I. Rodriguez-Iturbe, Multidimensional modeling of cumulative rainfall: Parameter estimation and model adequacy through a continuum of scales, *Water Resour. Res.*, 24(7), 985-992, 1988.
- Koepsell, R. W., J. B. Valdés, and J. F. Griffiths, Precipitation parameters for a multidimensional model of the Brazos Valley, paper presented at the ASCE Texas Section Fall Meeting, Am. Soc. Civ. Eng., College Station, Oct., 1988.
- Luenberger, D. G., *Introduction to Linear and Nonlinear Programming*, 2nd ed., Addison-Wesley, Reading, Mass., 1984.
- McConnell, A., and G. R. North, Sampling errors in satellite estimates of tropical rain, *J. Geophys. Res.*, 92, 9567-9570, 1987.
- Patterson, B. L., M. Hudlow, P. J. Pytlowany, F. Richard, and J. Hoff, GATE radar rainfall processing system, *Tech. Memo. EDIS 26*, Natl. Oceanic and Atmos. Admin., Washington D. C., May 1979.
- Shin, K.-S., and G. R. North, Sampling error study for rainfall estimate by satellite using a stochastic model, *J. Appl. Meteorol.*, 27(11), 1218-1231, 1988.
- Short, D., and G. R. North, The beam filling error in ESMR 5 observations of GATE rainfall, *J. Geophys. Res.*, this issue.
- Simpson, J. (Ed.), A satellite mission to measure tropical rainfall. Report of the Science Steering Group. NASA, Goddard Space Flight Cent., Greenbelt, Md., Aug. 1988.
- Simpson, J., R. F. Adler, and G. R. North, A proposed tropical rainfall measuring mission (TRMM) satellite, *Bull. Am. Meteorol. Soc.*, 69, 278-295, 1988.
- Valdés, J. B., I. Rodriguez-Iturbe, and V. K. Gupta, Approximations of temporal rainfall from a multidimensional model, *Water Resour. Res.*, 21(8), 1259-1270, 1985.
- Valdés, J. B., S. Nakamoto, S. S. P. Shen, and G. R. North, Satellite-based applications of the WGR model, paper presented at the AGU/AMS Conference on Mesoscale Precipitation: Analysis, Simulation and Forecasting, Mass. Inst. of Technol., Cambridge, Sept. 13-17, 1988.
- Waymire, E., and V. K. Gupta, The mathematical structure of rainfall representations, *Water Resour. Res.*, 17(5), 1275-1294, 1981.
- Waymire, E., V. K. Gupta, and I. Rodriguez-Iturbe, A spectral theory of rainfall intensity at the meso- β scale, *Water Resour. Res.*, 20(20), 1453-1465, 1984.
- S. Nakamoto and G. R. North, Climate System Research Program, Texas A&M University, College Station, TX 77843.
- S. S. P. Shen, Mathematics Department and Climate System Research Program, Texas A&M University, College Station, TX 77843.
- J. B. Valdés, Civil Engineering Department and Climate System Research Program, Texas A&M University, College Station, TX 77843.

(Received December 19, 1988;
revised May 22, 1989;
accepted May 31, 1989.)